RESEARCH ARTICLE
doi: 10.2306/scienceasia1513-1874.2011.37.240

ScienceAsia 37 (2011): **240–246**

Effects of sintering temperatures on micro-morphology, mechanical properties, and bioactivity of bone scaffolds containing calcium silicate

Lupong Kaewsichan[a], **Daungporn Riyapan**[a], **Phanida Prommajan**[a], **Jasadee Kaewsrichan**[b,*]

[a] Department of Chemical Engineering, Faculty of Engineering, Prince of Songkla University, Hat Yai, Songkhla, Thailand

[b] Department of Pharmaceutical Chemistry, Faculty of Pharmaceutical Sciences, Prince of Songkla University, Hat Yai, Songkhla, Thailand

*Corresponding author, e-mail: jasadee.k@psu.ac.th

Received 20 Dec 2010
Accepted 4 May 2011

ABSTRACT: In order to develop biomaterials for hard bone repair, biomimetic scaffolds were prepared from a mixture of hydroxyapatite (HA), β-tricalcium phosphate (TCP), and calcium silicate (CS) at optimal weight ratios via the sintering technique. Composites obtained had homogeneous pore distribution and open pore morphology. Depending on the amount of CS added and the sintered temperature, the porosity obtained varied in a range of 47–64%. The scaffolds flexural strength and modulus of the scaffolds were comparable to that of cancellous bone. Improved mechanical properties were achieved by introducing CS at elevated sintering temperature. Fine particles of CS are more resistant to heat than those of HA or TCP, which are larger in diameter. Integration of CS grains with the HA/TCP composite does not occur by sintering at 1250 °C. CS particles were mainly distributed at the composite grain boundaries, and played a role in cracking resistance. To test bioactivity in vitro, the scaffolds were immersed in phosphate buffered saline for 3 weeks, and then assessed for apatite forming ability. Apatite did not form on the scaffolds sintered at 1050 and 1150 °C, but it did in those sintered at 1250 °C. The new biomaterials produced are suitable to prepare scaffolds, which may be used for long bone tissue engineering.

KEYWORDS: load-bearing scaffold, bioactive ceramics, apatite layer, hydroxyapatite

INTRODUCTION

Tissue engineering aims to develop biological substitutes by incorporating cells and/or growth factors into a three-dimensional scaffold to mimic native tissue architecture and function[1]. A common approach is to isolate specific cells through a small biopsy from a patient and then let them grow on a scaffold under controlled conditions. Bone defects or voids, as induced by traumatic injury, orthopedic surgery, and tumour resection, require bone replacement. Autologous bone grafting is the gold standard in reconstructive surgery owing to its high immunocompatibility. However, the technique is bound by several constraints relating to the requirement of a secondary surgery, limited amount of tissue to be harvested, and increased risk of infection or recurrent pain[2]. Bone tissue engineering is thus emerging to overcome these problems.

The challenge faced by the field of tissue engineering is that the physico-chemical nature of the material surface and the biological behaviour of the cells should match in a sequestered pattern to form a functional tissue. Therefore, in selecting the correct biomaterials properties such as surface topography, chemical composition, hydrophilicity, surface energy and charge, and degradation should be carefully considered. A range of bioactive ceramics such as hydroxyapatite (HA), tricalcium phosphate (TCP), bioglass, and glass ceramics have been employed because of their similarities in composition to the mineral phase of natural bone and their excellent bone bonding ability[3]. So far, the applications as long bone substitute and load-bearing scaffolds are hindered by the low intrinsic strength exhibited by HA. Dense HA displays fracture toughness slightly below the lower limit of cortical bone[4]. Conversely, Young's modulus is typically higher[5] and the flexural strength is limited to ∼80 MPa[6]. To improve the mechanical features of load-bearing scaffolds, HA-based composite materials have been developed. It is important to reach an equilibrated biomechanical load distribution at the bone/scaffold interface, and to reduce strength mismatch favourable for osseous tissue integration. For example, a low melting point

bioceramic, TCP, has been used to supplement HA, resulting in increased flexural strength and degradability of the composite scaffolds[7]. A series of different compositions have been investigated, e.g., HA plus ZrO_2[8], HA plus Al_2O_3, and other mixtures with high thermal resistance[9]. However, a problem of phase decomposition has arisen, mainly caused by chemical interactions between HA and the reinforcing phases at high temperatures. Although high thermal stability of the reinforcing phases enhances the mechanical resistance of the composite, forming of secondary phases results in volume modification, which in turn induces micro-cracks in the final product[10].

Success in orthopedic applications is also limited by poor resorption of HA. In contrast to the perfectly stoichiometric compound HA [$Ca_{10}(PO_4)_6(OH)_2$], bone mineral has a defective structure, being doped with mono- or divalent cations [BM, $Ca_{10\text{-}x}(HPO_4)_x(PO_4)_{6\text{-}x}(OH)_{2\text{-}x}$]. As a result, their reabsorption is enhanced[11]. TCP and silicate-based bioceramics are better biodegradable materials than HA. Regarding bone regeneration capacity, the efficacy of scaffold products containing parts of these materials has been improved consequently[7,12,13]. For an HA/TCP hybrid surface, the ionic micro-environment established by partial dissolution of calcium phosphate from TCP crystals has been found optimal for apatite layer formation, which is appropriate for cell attachment, migration, and growth[7]. Silicate-based bioceramic products exhibit a surface chemistry amenable to extracellular matrix proteins. Silica, which acts as a nucleating apatite, in conjunction with strong protein films on the material that facilitated cell adhesion and other cellular activities promotes bone bonding in vivo[13]. Usually, they are selected as the reinforcing phases because of exhibiting higher flexural strength and reduced elastic modulus compared to HA[14].

The most important stage of bone tissue engineering is the design and processing of porous, biodegradable 3D scaffolds. The scaffolds should provide structural support for cells and newly formed tissues by acting as a temporary extracellular matrix for natural processes of tissue regeneration and development, while degrade at a rate comparable with new tissue growth[15]. Scaffold porosity needs to be determined to ensure adequate space for cell migration and expansion, and suitable transport of nutrients and waste products[16,17]. To improve the criteria required for successful bone grafting, the logical approach is to use the properties of more than one material to combine the strength of the parent phases and simultaneously minimize any undesirable characteristics.

According to our previous study, improved osteoconductivity in vivo has been apparent for composite scaffolds consisting of HA and TCP at 2:1 mass ratio in comparison with TCP implants[7]. In this work, variable amounts of calcium silicate (CS) were supplemented into the prescribed composite materials to investigate the role of the reinforcing phase on determining the mechanical properties and bioactivity of the finished scaffold products in vitro. To date, there has been no report publishing the development of HA/TCP/CS composites for load-bearing applications.

EXPERIMENTAL METHODS

Scaffold preparation

The powders of HA (Fluka), TCP (Fluka), and CS (Riedel-de Haën) were approximately of 7.9, 4.7, and 0.8 μm in diameter, respectively. The mixed powder of HA and TCP at a mass ratio of 2:1 was prepared, and then blended with CS at a concentration range of 10–30% w/w. The sieved sucrose particles (400–600 μm in diameter) were added by keeping its content constant at 16.7% w/w, so that the scaffold porosity will match that of the long and/or load-bearing bones[18]. Polyvinyl alcohol solution (15% w/v) was used as a wetting agent for granule preparation. The dried granules were poured into a mould and pressed with a constant load of hydraulic press. The prepared samples were sintered at 1050 °C, 1150 °C, or 1250 °C for 2 h.

Physical characterization of scaffolds

Scanning electron microscope (SEM) (Quanta 400, FEI, Czech Republic) was used to characterize surface morphology, pore shape and size, and pore distribution of scaffolds after gold coating.

The initial modulus and flexural strength were evaluated via three-point bending tests on a universal testing machine (LLOYD, West Sussex, UK). These studies were conducted on a scaffold of dimensions 25 mm × 60 mm × 9 mm according to BSEN ISO 14125:1998. A cross-head speed of 1 mm/min was used with a 1 kN load cell. The strength and modulus were calculated from the maximum load recorded. Three samples were examined for each condition.

Porosity of scaffolds

The Archimedes method was used to measure the porosity of porous ceramic scaffolds in water. The dry weight of each scaffold was recorded as m_1. Then, the scaffold was immersed in water until no bubbles emerge. The sample was reweighed in water

to measure m_3. After that, the scaffold was carefully taken out the beaker, and the surface water droplets were dabbed off. The sample was quickly reweighed in air to measure m_2. Three samples were tested to calculate the average porosity. The porosity of the open pores within the scaffold was calculated as $(m_2 - m_1)/(m_2 - m_3)$.

Soaking in PBS

The phosphate buffered saline (PBS) solution was prepared by dissolving 80 g NaCl, 2 g KCl, 14.4 g Na_2HPO_4, and 2.4 g KH_2PO_4 in a litre of water, and the pH adjusted to 7.4 [19]. Triplicate samples from each group of scaffolds were immersed in 20 ml PBS for 3 weeks at 37 °C without stirring. After removal, the sample was gently washed with deionized water, and dried at room temperature. The corresponding non-immersed scaffold served as the control. SEM was performed to examine surface characteristics of the scaffolds after soaking.

Statistical analysis

All data are expressed as mean ± standard deviations of experiments carried out in triplicate. Statistical analyses were performed with SIGMA PLOT software. Student's t-test was used to determine the significant differences among the groups, and p-values less than 0.05 were considered significant.

RESULTS

Morphology and microstructure of scaffolds

Fig. 1 shows the interior morphology and microstructure of porous scaffolds fabricated under different conditions. The scaffolds contain CS in concentrations of 10% (a and d), 20% (b and e), and 30% (c and f). Scaffolds were sintered at 1050 °C (Fig. 1a–c) or 1250 °C (Fig. 1d–f) for 2 h. All of the scaffolds produced exhibited opened, interconnected, and homogeneous pore structures with irregular pores of 5–20 μm diameter. The pore interconnectivity was estimated to arise from the contact points between adjacent crystals of HA and/or TCP, which were larger in particle size than those in CS, and resulted from the burning out of sucrose and PVA solution (Fig. 1d–f). The ceramic grains were not molten at the lower sintered temperature of 1050 °C (Fig. 1a–c), and distinct particle morphologies were clearly observed. The grains, in particular of HA and TCP, became molten at the higher sintered temperature of 1250 °C (Fig. 1d–f). In addition, by increasing CS contents, the uniform distribution of CS was still noticed. Alteration of the pore structure was not detected by the addition of CS into the HA/TCP mixture (Fig. 1d–f).

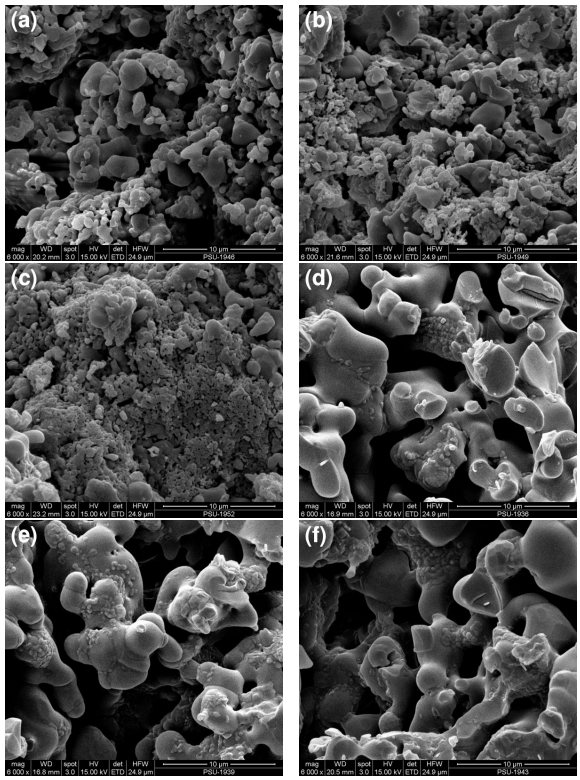

Fig. 1 SEM micrographs of scaffolds fabricated under different conditions. The CS powder with increased concentrations, e.g., 10% (a and d), 20% (b and e), and 30% (c and f), was blended with the composite powder of HA and TCP (2:1 mass ratio) to form the scaffolds. Then, they were sintered at 1050 °C (a, b, and c) or 1250 °C (d, e, and f) for 2 h.

Flexural properties and porosity

For scaffold samples being sintered at similar temperature, the flexural strength and modulus were increased by increasing the CS contents (Table 1). For the scaffolds containing identical CS concentrations, increasing the sintered temperature improved the flexural properties (Fig. 2). The porosity was reduced from 64% to 47% as the results of increased CS concentrations and sintered temperature. It is worth noting that strength and modulus of the composites slightly increased when the percentage of CS, the sintered temperature, or both were elevated, albeit decreasing the porosity.

Apatite formation in PBS

Fig. 3 presents the most relevant SEM micrographs for CS containing scaffolds sintered at 1050 °C (a and b), 1150 °C (c and d), and 1250 °C (e and f) 3 weeks after immersion in PBS. Scaffolds comparison before

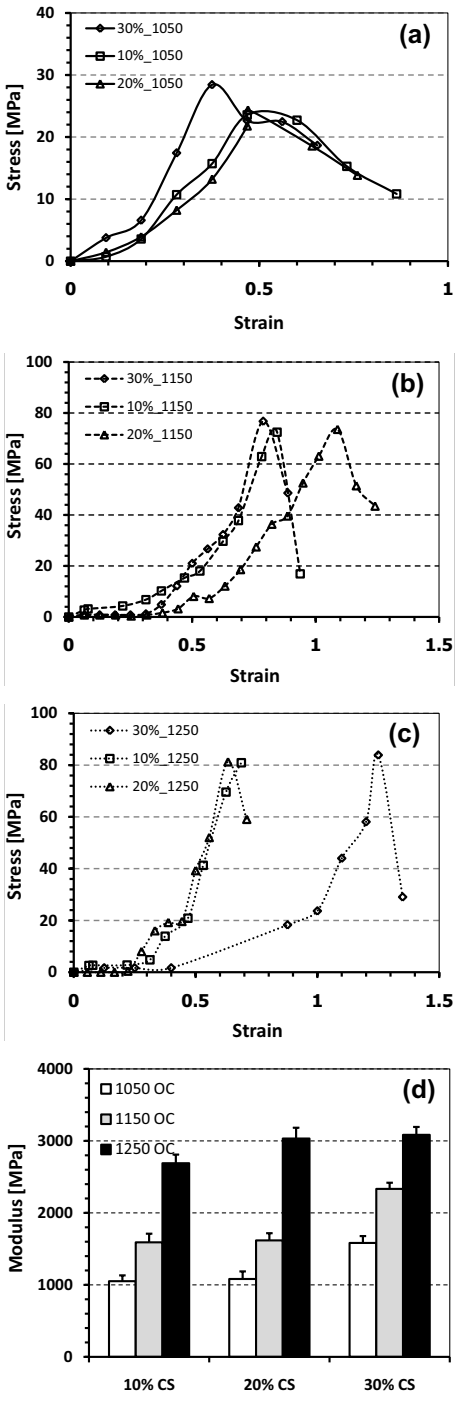

Fig. 2 Stress-strain curves of the scaffolds consisting of varying CS concentrations sintered at (a) 1050 °C, (b) 1150 °C, or (c) 1250 °C, and (d) the values of flexural modulus calculated from the curves. Bars represent mean ± standard deviation. Statistical analysis indicated that the composite materials prepared by using different %CS and/or sintered temperature had significant different physical behaviours.

Table 1 Composition of the scaffolds as HA+TCP(2:1):CS (% w/w), sintering temperature T, calculated flexural strength σ, flexural modulus E, and porosity ϕ.

Name	Comp.	T (°C)	σ (MPa)	E (GPa)	ϕ (%)
F1	90:10	1050	4.9 ± 0.06	1.05 ± 0.02	63.7
F2	80:20	1050	5.1 ± 0.08	1.08 ± 0.02	62.9
F3	70:30	1050	5.9 ± 0.12	1.58 ± 0.05	61.4
F4	90:10	1150	13.1 ± 0.21	1.59 ± 0.01	57.6
F5	80:20	1150	16.5 ± 0.11	1.62 ± 0.01	54.6
F6	70:30	1150	17.3 ± 0.18	2.33 ± 0.06	52.7
F7	90:10	1250	17.3 ± 0.24	2.69 ± 0.04	52.1
F8	80:20	1250	23.8 ± 0.32	3.03 ± 0.02	50.3
F9	70:30	1250	38.5 ± 0.44	3.08 ± 0.02	47.1

(Fig. 3a, 3c, and 3e) and after (Fig. 3b, 3d, and 3f) soaking indicates that immersion in PBS resulted in the formation of rougher surfaces when the scaffolds were sintered at 1050 and 1150 °C (Fig. 3b and 3d). Interestingly, spherical granules in densely packed needle-like crystals appeared for the immersed scaffolds sintered at 1250 °C (Fig. 3f).

DISCUSSION

The substitution of long and load-bearing bone segments is one of the most relevant challenges of orthopaedic surgery with enormous societal and economical impact. The optimal solution to face this challenge is the development of bioactive porous scaffolds, able to promote the formation of new bone tissue and to sustain the mechanical load during bone regeneration processes. In this study, the sintering technique was applied to fabricate scaffolds for obtaining the consolidation of composite bodies (HA/TCP) and a reinforcing phase (CS). A median pore diameter of approximately 15 μm with homogeneous distribution was apparent (Fig. 1). The particle sizes of sucrose were several times larger than the pore diameter observed, suggesting that pores coalesce during sintering. The prepared scaffolds showed well-interconnected pores with a porosity in the range of 47–64%, depending on the amount of CS added and the sintered temperature. The porosity diminished when higher concentrations of CS and high sintered temperature were used. Consequently, it was optimal for placing the scaffolds somewhere between cortical and cancellous bones that create a porous environment with 3–12% and 50–90% porosity, respectively[20]. The scaffold attained a minimal flexural strength of 5 MPa, which was comparable to the strength of cancellous bone (2–10 MPa)[21]. The modulus at 50% porosity (3 GPa) showed a 3-fold increment

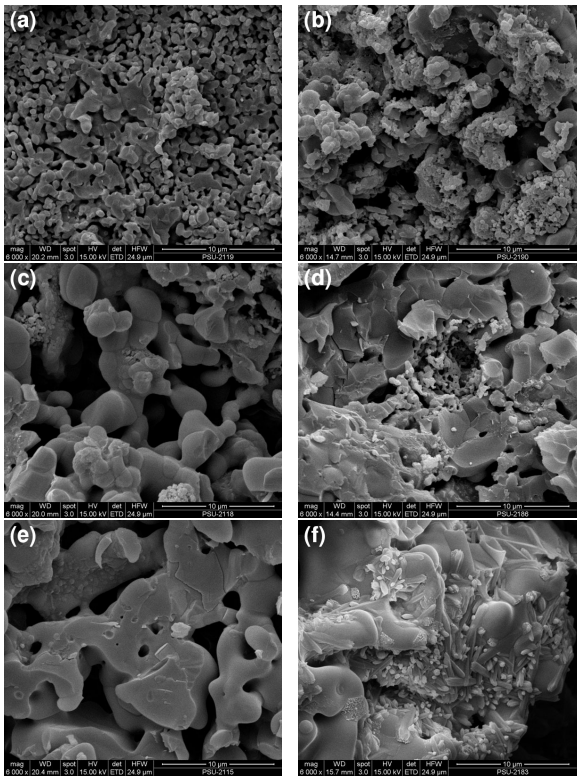

Fig. 3 SEM images of CS containing scaffolds before and after soaking in PBS for 3 weeks. The scaffolds were sintered at different temperatures: 1050 °C (a and b), 1150 °C (c and d), and 1250 °C (e and f). (a), (c), and (e): before soaking; and (b), (d), and (f): after immerging.

when changing the sintered temperature from 1050 to 1250 °C (Table 1). Significant improvement in the mechanical properties was consequently accomplished by introducing CS in the scaffold formulations and/or elevating the sintered temperature.

The microstructures of the scaffolds seem to be influenced by heating levels used upon fabrication. Not all ceramic grains were molten at 1050 °C, as different particle morphologies were clearly observed (Fig. 1a–c). Fusion of the grains, especially between HA and/or TCP, was revealed at 1150 °C (Fig. 3c), while these materials were completely molten at 1250 °C (Fig. 1d–f). However, integration of the CS grains with the composite bodies was not accomplished by the last temperature level, suggesting a high thermal resistance of the reinforcing phase. CS was thoroughly distributed although its concentration was increased up to 30% w/w, indicating a well controlled mixing process. It was recognized that CS particles were approximately 10 and 5 times smaller in diameter than HA and TCP, respectively, (Fig. 1),

Table 2 Ion concentrations of human blood plasma, SBF, and PBS.

Type	Ion concentration (mM)						
	Na^+	K^+	Mg^{2+}	Ca^{2+}	Cl^-	HCO_3^-	HPO_4^{2-}
Blood plasma	142.0	5.0	1.5	2.5	103.0	27.0	1.0
SBF	142.0	5.0	1.5	2.5	148.8	4.2	1.0
PBS	157.0	4.5	–	–	140.0	–	10.0

and the distribution of CS was found dominantly at the composite grain boundaries (Fig. 3e). In agreement with the improved mechanical properties by the addition of CS, the boundary distribution was expected to play an important role in microcracking. The results were consistent with the previous study, suggesting that smaller grains have stronger cracking resistance, which in turn affects the strength of the ceramic composites as a whole[22].

The simulated body fluid (SBF) method has been suggested as a useful way for testing bioactivity of bioceramics in vitro by assessing the potential of apatite formation[4]. Silicate-based bioceramics, including bioglass[4], wollastonite ($CaSiO_3$)[23], akermanite ($Ca_2MgSi_2O_7$)[24], and diopside ($Ca_2MgSi_2O_6$)[25], have been shown to have excellent apatite forming abilities in SBF. However, by soaking phosphate- and sulphate-based ceramics in SBF, obvious apatite formation has not been remarkable, although they do exhibit superior in vivo bone formation abilities[26]. Therefore, SBF has been suitable for evaluating the in vitro bioactivity of silicate-based ceramics, but not for other types of bioceramics. Indeed, the bone bonding ability of biomaterials depends on their chemical reactivity in body fluid[27]. Phosphate buffered saline (PBS) is another physiologic solution commonly used in biochemistry to imitate human extracellular fluid. In comparison to SBF, ionic species such as Mg^{2+}, Ca^{2+}, and HCO_3^- are absent in PBS (Table 2). SBF ionic strength is similar to that of blood plasma. In the present study, we used PBS instead of SBF to ascertain the ability of inducing apatite formation on the immersed scaffolds. By soaking the scaffolds previously sintered at 1050 and 1150 °C in PBS for 3 weeks, more bumpy surfaces were apparent on which the apatite layer was not detected (Fig. 3b and d). However, the deposition of spherical-like granules of CS[28] and needle-like crystals of HA[29,30] was demonstrated on the soaked scaffolds being sintered at 1250 °C (Fig. 3f). The ability of biomaterials to form apatite in PBS depends on the heating challenge that fully induces the grain transformation. These results

contradict those reported previously, indicating that the formation of bone apatite on fully sintered HA and TCP ceramics has been hardly detectable[31,32]. Indeed, the nature and crystallinity of apatite forming phases depend on various parameters, including concentrations of phosphate/carbonate sources, ionic strength and pH of the soaked solution, and the kinetics of the nucleation and growth processes[33]. Because the porosity of the scaffolds was not compromised by the formed apatite layers and the initial porous morphology was maintained, the composites produced in this study are potential candidates to be used as new biomaterials for hard tissue repair.

Acknowledgements: The financial support of this work was obtained from the Discipline of Excellence in Chemical Engineering, Department of Chemical Engineering, Faculty of Engineering, Prince of Songkla University.

REFERENCES

1. Langer R, Vacanti JP (1993) Tissue engineering. *Science* **260**, 920–6.
2. Arosarena O (2004) Tissue engineering. *Curr Opin Otolaryngol Head Neck Surg* **13**, 233–41.
3. Wang M (2003) Developing bioactive composite materials for tissue replacement. *Biomaterials* **24**, 2133–51.
4. Hench LL (1991) Bioceramics: from concept to clinic. *J Am Ceram Soc* **74**, 1487–510.
5. Hench LL (1998) Bioceramics. *J Am Ceram Soc* **81**, 1705–28.
6. Kothapali C, Wei M, Shaw MT (2004) Influence of temperature and concentration on the sintering behavior and mechanical properties of hydroxyapatite. *Acta Mater* **52**, 5655–63.
7. Wongwitwichot P, Kaewsrichan J, Chua KH, Ruszymah BHI (2010) Comparison of TCP and TCP/HA hybrid scaffolds for osteoconductive activity. *Open Biomed Eng J* **4**, 279–85.
8. Sung YM, Shin YK, Ryu JJ (2007) Preparation of hydroxyapatite/zirconia bioceramic nanocomposites for orthopaedic and dental prosthesis applications. *Nanotechnology* **18**, 65602–7.
9. Chiba A, Kimura S, Raghukandan K, Morizono Y (2003) Effect of alumina addition on hydroxyapatite biocomposites fabricated by underwater-shock compaction. *Mater Sci Eng A* **350**, 179–83.
10. Sprio S, Tampieri A, Celotti G, Landi E (2009) Development of hydroxyapatite/calcium silicate composites addressed to the design of load-bearing bone scaffolds. *J Mech Behav Biomed Mater* **2**, 147–55.
11. Tas AC, Bhaduri SB (2004) Rapid coating of Ti6A14V at room temperature with a calcium phosphate solution similar to 10x simulated body fluid. *J Mater Res* **19**, 2742–9.
12. Ng AM, Tan KK, Phang MY, Aziyati O, Tan GH, Isa MR, Aminuddin BS, Naseem M, Fauziah O, Ruszymah BH (2008) Differential osteogenic activity of osteoprogenitor cells on HA and TCP/HA scaffold of tissue engineered bone. *J Biomed Mater Res A* **85**, 301–12.
13. Hing KA,Revell PA, Smith N, Buckland T (2006) Effect of silicon level on rate, quality and progression of bone healing within silicate-substituted porous hydroxyapatite scaffolds. *Biomaterials* **27**, 5014–26.
14. Gou Z, Chang J (2004) Synthesis and in vitro bioactivity of dicalcium silicate powders. *J Eur Ceram Soc* **24**, 93–9.
15. Lee SH, Shin H (2007) Matrices and scaffolds for delivery of bioactive molecules in bone and cartilage tissue engineering. *Adv Drug Deliv Rev* **59**, 339–59.
16. Chaignaud BE, Langer R, Vacanti JP (1997) The history of tissue engineering using synthetic biodegradable polymer scaffolds and cells. In: Atala A, Mooney DJ (eds) *Synthetic Biodegradable Polymer Scaffolds*, Birkhauser, Boston, MA.
17. Thompson RC, Wake MC, Yasemski MJ, Mikos AG (1995) Biodegradable polymer scaffolds to regenerate organs. *Adv Polymer Sci* **122**, 245–74.
18. Cowin SC (1989) *Bone Mechanics Handbook*, 2nd edn, Boca Raton, CRC Press, New York.
19. Sambrook J, Fritsch EF, Maniatis T (1989) *Molecular Cloning: A Laboratory Manual*, 2nd edn, Cold Spring Harbor Laboratory Press, Cold Spring Harbor, New York.
20. Cooper DM, Matyas JR, Katzenberg MA, Hallgrimsson B (2004) Comparison of microcomputed tomographic and microradiographic measurement of cortical bone porosity. *Calcif Tissue Int* **74**, 437–47.
21. Santin M, Morris C, Standen G, Nicolais L, Ambrosio L (2007) A new class of bioactive and biodegradable soybean-based bone fillers. *Biomacromolecules* **8**, 2706–11.
22. Pezzotta M, Zhang ZL (2010) Effect of thermal mismatch induced residual stress on grain boundary microcracking of titanium diboride ceramics. *J Mater Sci* **45**, 382–91.
23. Wu C, Ramaswamy Y, Kwik D, Zreiqat H (2007) The effect of strontium incorporation into $CaSiO_3$ ceramics on their physical and biological properties. *Biomaterials* **28**, 3171–81.
24. Wu C, Chang J, Ni S, Wang J (2006) In vitro bioactivity of akermanite ceramics. *J Biomed Mater Res A* **76**, 73–80.
25. Iwata NY, Lee GH, Tokuoka Y, Kawashima N (2004) Sintering behavior and apatite formation of diopside prepared by coprecipitation process. *Colloids Surf B Biointerfaces* **34**, 239–45.
26. Liu G, Zhao L, Cui L, Liu W, Cao Y (2007) Tissue-engineered bone formation using human bone marrow stromal cells and novel β-tricalcium phosphate. *Biomed Mater* **2**, 78–86.
27. Xue W, Liu X, Zheng X, Ding C (2005) In vivo evaluation of plasma-sprayed wollastonite coating. *Biomaterials* **26**, 3455–60.

28. Leonor IB, Balas F, Kawashita M, Reis RL, Kokubo T, Nakamura T (2006) Biomimetic apatite formation of different polymeric microsphere modified with calcium silicate solutions. *Key Eng Mater* **309-311**, 279–82.
29. Yao X, Yao H, Li G, Li Y (2010) Biomimetic synthesis of needle-like nano-hydroxyapatite template by double-hydrophilic block copolymer. *J Mater Sci* **45**, 1930–6.
30. Liao JG, Zuo Y, Zhang L, Li YB, Wang YL (2009) Study on bone-like nano-apatite crystals. *J Funct Mater* **40**, 877–80.
31. Balas F, Perez-Pariente J, Vallet-Regi M (2003) In vitro bioactivity of silicon-substituted hydroxapatites. *J Biomed Mater Res A* **66**, 364–75.
32. Kim HM, Himeno T, Kawashita M, Kokubo T, Nakamura T (2004) The mechanism of biomineralization of bone-like apatite on synthetic hydroxyapatite: an in vitro assessment. *J R Soc Interface* **1**, 17–22.
33. Sahai N (2005) Modeling apatite nucleation in the human body and in the geochemical environment. *Am J Sci* **305**, 661–72.